CHEMICAL ENGINEERING TRANSACTIONS, Volume 16, 2008
Guest Editor Eliseo Ranzi
 ISBN 978-88-95608-03-7 ISSN 1974-9791

Sooting Propensity Of Gasoline And Biofuel Droplets

A. Cuoci, A. Frassoldati, T. Faravelli, E. Ranzi
Dipartimento di Chimica, Materiali e Ingegneria Chimica, Politecnico di Milano
P.zza Leonardo da Vinci n. 32, 20133 Milano, Italy

This paper discusses the effect of ethanol addition on soot formation during the combustion of gasoline droplets. The numerical modeling of spherically-symmetric droplet combustion is performed by solving the gas and liquid phase conservation equations of mass, species, and energy with the proper initial and boundary conditions. Non-ideal vapour-liquid equilibria are considered taking into account water condensation in the fuel droplet. The model also includes radiative heat transfer, also incorporating continuum radiation from soot particles. A general, detailed chemical reaction mechanism, consisting of ~5000 reactions involving ~300 molecular and radical species, is used to describe the gas phase pyrolysis, oxidation and combustion of hydrocarbons, including PAH formation reactions. This mechanism allowed to analyze and discuss the positive effect of ethanol addition and also the negative influence on soot formation of the initial presence of aromatics in the fuel.

1. Introduction

In the last years new factors are changing the energy strategy and especially the fuel demand. From one side the recent dramatic increase of the crude oil barrel cost is pushing toward alternative sources. The second and more important aspect refers to the environmental impact of fossil fuels on the global warming. Kyoto protocol fixed the parameters for the next decades in terms of CO_2 emission of each country.
Transportation gives a significant contribution to the greenhouse effect. For this reason car companies have been working on increasing the engine efficiencies. Together with this effort, the new strategies address the attention to the renewable fuels, which can answer to both the demands: reduction of the oil dependency and control of CO_2. In this context ethanol is nowadays playing an important role. Ethanol comes from the fermentation of sugars contained in many biomasses and shows quite good properties to be used in conventional internal combustion engines: it is an octane number enhancer and stands as a candidate for conventional transportation fuel replacement. Moreover, ethanol is an oxygen carrier, and oxygen content in the automotive fuels allows a reduction of the emission and in particular of carbon monoxide and soot. In order to quantify this positive effect on particulate emission, this work compares the model results of soot formation coming from the combustion of different liquid droplets of gasoline surrogates containing also ethanol. The choice of an isolated droplet lies in the need of investigating the chemistry of combustion and pollutant formation of a liquid fuel, but avoiding the complexities of the

Please cite this article as: Cuoci A., Frassoldati A., Faravelli T. and Ranzi E., (2008), Sooting propensity of gasoline and biofuel droplets, Chemical Engineering Transactions, 16, 233-240

physical phenomena coming from the interactions among the droplets of a spray. Moreover, experimental data of the sooting behaviour of an isolated droplet of ethanol obtained under microgravity conditions are available (Yozgatligil et al., 2004 and Urban et al., 2004).
The compared gasoline is surrogated by Primary Reference Fuels (PRF), i.e. by a mixture of n-heptane and iso-octane and by a so called Toluene Reference Fuel (TRF), in which toluene is added to PRF (Pitz et al., 2007). The need to resort to these surrogates is because of the complexity of gasoline, which is a mixture of hundreds of components. PRF are already commonly used to measure the antiknock propensity of gasoline through the octane number. Ternary, and eventually larger surrogates, intend to investigate the effects of chemical composition on internal combustion engine efficiency and emission. Toluene is the most prevalent aromatic in gasoline (up to 35% wt) and for this reason it is generally assumed to represent the whole aromatic class. The importance of including aromatics in the gasoline surrogate lies in their refractoriness to the autoignition, because of their strong stability. Moreover, toluene and alkyl-aromatics in general form phenyl-like radicals, which are resonantly stabilized. These long living radicals scavenge other reactive radicals with a global reduction of the autoignition properties of the mixture. Finally, and of interest for the present work, aromatics are precursors of soot formation and their presence increase the propensity of the fuel to form carbonaceous particulate matter.

2. Mathematical model

The evaporation and combustion of spherically-symmetric liquid droplets is modeled through conservation equations of mass, species, and energy with the proper initial and boundary conditions. Non-ideal vapor-liquid equilibrium is considered taking into account water condensation/vaporization at the droplet surface. The model originally proposed by (Cuoci *et al.*, 2005a) is here extended for describing multicomponent liquid fuels through the Stefan-Maxwell theory (Krishna *et al.*, 1993). In the following only the extension to multicomponent diffusion in the liquid phase is briefly discussed. Details can be found in (Cuoci *et al.*, 2005b). In the species conservation equations the mass diffusion fluxes j_i^L can be calculated according to the Stefan-Maxwell theory:

$$j_i^L = \sum_{k=1}^{NC_L} \left(B_{i,k}^{om} \cdot j_{L,k}^u \right) \quad \text{where} \quad B_{i,k}^{om} = \delta_{i,k} - \omega_i^L \left(1 - \frac{\omega_{NC_L}^L x_k}{x_{NC_L} \omega_k^L} \right) \tag{1}$$

The mass diffusion fluxes can be related to the molar diffusion fluxes through:

$$c_{tot}^L x_i j_{L,i}^u = \rho_L \omega_i^L J^L \qquad \underline{J_L} = -c_{tot}^L [D] \cdot [\Gamma] \underline{\left(\frac{\partial x_L}{\partial r} \right)} \tag{2}$$

where $\delta_{i,k}$ is the Kronecker delta, x_k are the mole fractions, c_{tot}^{L} is the total concentration; $\underline{J_L}$ and $\underline{\left(\partial x_L / \partial r\right)}$ are vectors containing the molar fluxes and the compositions gradients; The matrices $[D]$ and $[\Gamma]$ account for diffusion resistance and non-ideal liquid mixture:

$$\Gamma_{i,j} = \delta_{i,j} + x_i \left(\frac{\partial \ln \gamma_i}{\partial x_i} \right)_{T,P,k,k \neq j,k \neq NCL} \tag{3}$$

$$[D] = [B]^{-1} \qquad \text{where} \qquad \begin{cases} B_{i,k} = -x_i \left(\dfrac{1}{D_{i,k}} - \dfrac{1}{D_{i,NC_L}} \right) \\ B_{i,i} = \dfrac{x_i}{D_{i,NC_L}} + \displaystyle\sum_{\substack{j=1 \\ j \neq i}}^{NC_L} \frac{x_j}{D_{i,j}} \end{cases} \tag{4}$$

In the expressions reported above $D_{i,k}$ are Stefan-Maxwell diffusivities (Krishna *et al.*, 1993), γ_i the activity coefficients (calculated using the Wilson model (Reid *et al.*, 1988)).

The analytical solution proposed by (Kazakov *et al.*, 2003) is used to describe the heat flux due to the non-luminous radiative heat transfer in the gas phase. This model includes radiative heat transfer only from the gas molecules CO, CO_2 and H_2O. Continuum radiation from soot particles was also incorporated assuming soot Planck mean contribution (Sazhin, 1994). For soot particles the thermophoretic effect is also considered, according to the approach proposed in (Gomez *et al.*, 1993).

The mathematical modeling of the combustion of fuel droplets gives rise to a system of partial differential equations which are transformed in a DAE system by using finite difference approximations. A specifically conceived numerical solver allows efficient treatment of the structured sparsity of the Jacobian matrix as well as the stiffness of the DAE system (Buzzi-Ferraris *et al.*, 1998; Buzzi-Ferraris, 2007).

3. Sooting propensity of fuel droplets

The broad multicomponent nature of gasolines and biofuels is compatible neither with reproducible experiments, nor with viable model simulations. Therefore it is convenient to use surrogate mixtures able to correctly describe the physical and chemical properties of the real fuels. In general, surrogate fuels are defined in order to reproduce density, thermal conductivity, heat capacity, viscosity and volatility of the fuel, and/or also ignition temperature, oxidation and burning rates, sooting propensity, etc.

Three different surrogate mixtures were investigated in the present work. Their composition is reported in Table 1. The PRF95 surrogate is a mixture of iso-octane and n-heptane and it is used as the main component in the remaining two surrogates, which are obtained mixing 80% of PRF95 with 20% of toluene (TRF95) or ethanol (ETRF95).

The mathematical model described in the previous section was applied to single fuel droplets having initial diameter of 2.5 mm burning in cold air at the initial temperature of

298K. In line with the approach proposed by (Marchese *et al.*, 1999), ignition was simulated by assuming a short period (~1 s) of pure evaporation at ambient temperature, followed by a non-uniform temperature radial profile peaking at ~1600K. After the ignition, a diffusive, spherically symmetric flame arises around the droplet, whose temperature begins to increase leading to the evaporation of fuel in the gas phase. The flame is sustained by the fuel mass flux associated to the vaporization. As a consequence the droplet diameter decreases up to the total consumption of the droplet. In Figure 1 the squared droplet diameter is reported versus the time for the ETRF95 surrogate burning at atmospheric pressure. It is easy to recognize that the squared diameter varies linearly with the time, following the well known d^2-law. The slope of this curve measures the vaporization rate, which results ~0.75 mm^2/s. The droplet can be considered totally consumed after 7-8 seconds. In the same Figure the flame diameter (defined as the location of peak temperature), is reported. It is possible to observe that, during the first phase of combustion, the flame diameter increases, moving towards larger distances from the droplet surface. In the second phase, since the droplet diameter becomes smaller and smaller, the flame positions moves towards locations closer to the droplet surface. A similar trend was also observed for the PRF95 and TRF95.

Figure 2 shows an example of model predictions in terms of radial profiles of temperature and main species around the droplet at two different times. The maximum temperature, initially located very close to the droplet, moves toward larger standoff ratios since the flame zone spreads due to the diffusion and the convective phenomena associated to the vaporization fluxes from the droplet. The mass fraction profiles of main species follow a similar trend and a typical diffusive burning regime is then observed. Pyrolysis conditions (high temperatures accompanied by large carbon species concentrations) exist inside the flame. The concentration of ethanol and iso-octane at the interface is dictated by vapour-liquid equilibrium and rapidly decreases to zero in the pyrolytic region, well before the maximum temperature. It is evident that O_2 becomes zero where the maximum temperature is reached and the main products are H_2O, CO, and CO_2. Figure 3 shows the predicted concentration profiles of acetylene, major aromatic species (i.e. benzene, naphthalene and pyrene) and soot. At 0.05 s the amount of soot and soot precursors is very low, because the

Surrogate	Composition (% Vol.)
PRF95	95% iso-octane 5% n-heptane
TRF95	80% PRF95 20% toluene
ETRF95	80% PFR95 20% ethanol

Table 1. *Composition of surrogates*

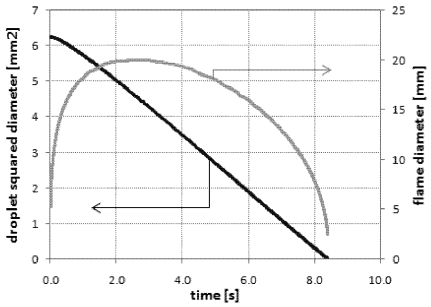

Figure 1. *Squared droplet diameter and flame diameter versus the time (ETRF95 surrogate, P=1atm).*

formation of such species is ruled by slow successive reactions; on the contrary the mass fraction of C_2H_2 is larger due to its chemistry relatively fast. At 5 s the profiles becomes very different: while the peak value of C_2H_2 remains roughly the same, aromatic species and especially soot show a strong increase, both in terms of peak value and total amount. Moreover the formation of such species is located only on the rich side of the flame; the mass fraction profiles show a rapid decrease toward zero on the lean side, where the concentration of soot becomes negligible. As a consequence the sooting zone is much smaller than the flame zone. The relative spatial position of peak values of aromatic species is a clear indication of the relative characteristic times of their chemistry. It is evident that benzene has a peak closer to the flame than soot, whose chemistry is slower.

In Figure 4 the peak soot mass fractions of investigated surrogates are compared versus the time. The results clearly show the higher tendency to soot formation of TRF95 surrogate, which contains toluene. As expected, the addition of aromatic species increases the soot formation. On the contrary, when toluene is substituted with ethanol in the ETRF95 surrogate, it is possible to observe a strong decrease in the soot formation. These results can be observed in terms of soot peak mass fraction and soot total amount, which is obtained by integrating the soot mass fraction over the entire gas phase around the droplet (Figure 5). Both peak and integral values of soot have a maximum and tend to decrease towards zero

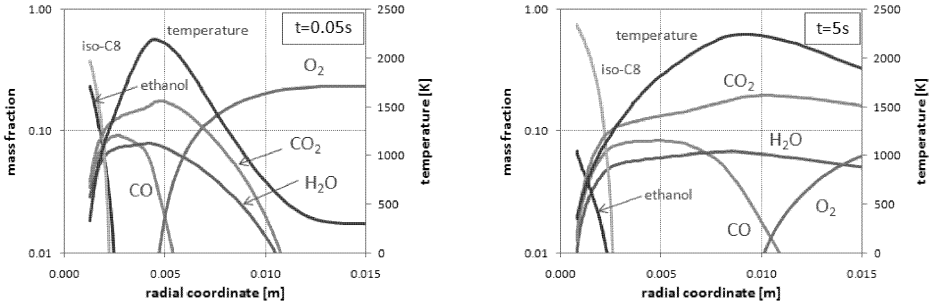

Figure 2. *Mass fraction profiles of temperature and main species along the non-dimensional radial coordinate (scaled on the droplet radius) for ETRF95 surrogate after 0.05 s and 5 s from ignition.*

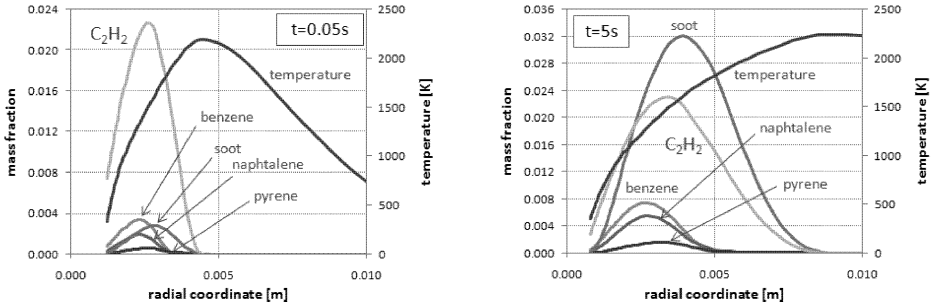

Figure 3. *Mass fraction profiles of soot and main soot precursors along the non-dimensional radial coordinate (scaled on the droplet radius) for ETRF95 surrogate after 0.05 s and 5 s from ignition.*

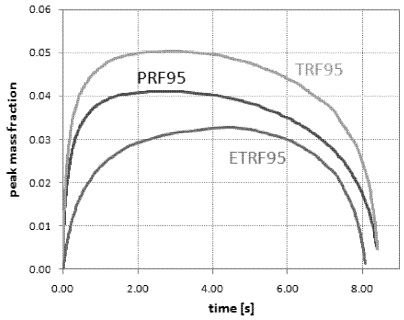

Figure 4. *Maximum of soot mass fraction versus time (P=1atm).*

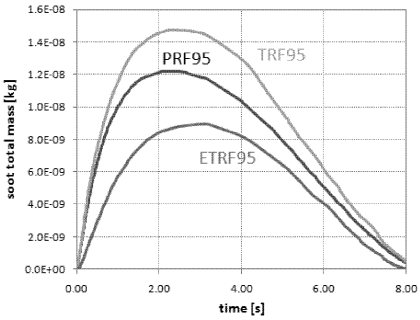

Figure 5. *Total mass of soot in the gas phase versus time (P=1atm).*

when the droplet diameter is sufficiently small. This can be explained by taking into account from one side the oxidation reactions which tend to consume soot and which are particularly strong in the lean side of the flame, where the oxygen concentration is high. On the other side it is necessary to consider the regression of droplet surface and the decrease in the fuel evaporation flux, which causes a progressive decrease in the amount of fuel which is supplied to the flame by the evaporating droplet.

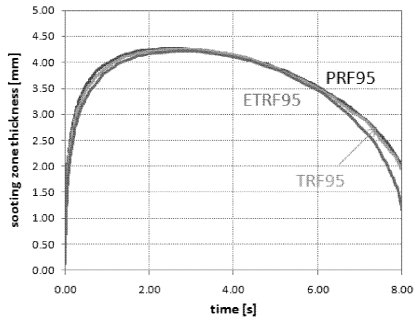

Figure 6. *Maximum of soot mass fraction versus time (P=1atm).*

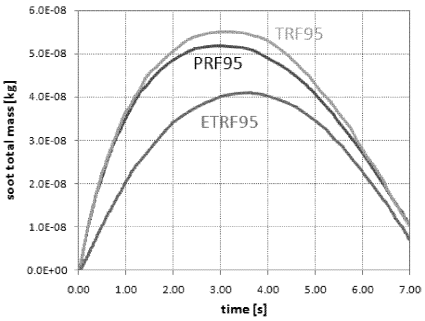

Figure 7. *Total mass of soot versus time (P=5atm).*

Figure 6 reports the thickness of the sooting zone versus the time for the three different surrogates. Despite the peak and total amount of soot are different, the thickness is practically the same for the surrogates, which seems to indicate that the sooting zone is mainly controlled by physical phenomena and is less influenced by the chemistry. The same analysis was repeated at 5 atm and the main results are reported in Figure 7. The higher soot propensity of TRF95 surrogate is confirmed also in this case, but the increase with respect to the PRF95 surrogate is less evident. Anyway, soot form ETRF95 decreases similarly to the case at 1 atm.

4. Kinetic analysis of the sooting propensity of different fuels

In order to better understand the different soot yields obtained from the combustion of different surrogates, it is useful to analyse the different fuels in ideal conditions. The formation of soot precursors is analysed in a plug flow reactor at 1500 K in air at Φ=2.

Figure 8 shows the benzene formation from n-heptane and iso-octane. Two different benzene peaks are clearly visible on this time log scale. The first one, at the very initial combustion stage, is mainly related to the formation of the first aromatic ring, due to propargyl radicals and C_3H_4 species. This first benzene formation is definitely higher in the case of iso-octane combustion, as clearly observed and discussed by (Pfefferle and McEnally 2003). This fact is even more evident when comparing propargyl radical formation from the two fuels. Branched alkanes and branched radicals favour isobutene and branched alkene formation with the final increase of propargyl radicals. The rapid and sharp decrease of this first benzene peak is due to the oxidation reactions of benzene (and phenyl radical). The second peak of benzene, in the post flame region, is mainly sustained by the successive reactions of acetylene following condensation reactions and HACA mechanism. Initial ethylene formation from n-heptane is clearly larger than the corresponding one from iso-octane, while the difference in acetylene mole fractions becomes less important, as clearly shown in Figure 9. This fact explains the similar behaviour of the *'secondary'* benzene formation. Successive formation of coronene is similar for both reference fuels.

As expected, similar trends are observed for the gasoline PRF95. On the contrary, a different behaviour is predicted when considering the surrogate mixture TRF95 containing also toluene. Figures 10 and 11 compare predicted mole fractions of soot precursors from TRF95 and PRF95. The initial benzene peak is higher in the case of TRF95 due to toluene de-methylation. This larger presence of benzene (and aromatics) persists in the post flame region and allows to explain the larger formation of coronene (first index of soot formation). Note that acetylene yields are very similar from both the surrogates.

On the contrary, the addition of 20% of ethanol to the surrogate PRF95 slightly reduces the initial formation of benzene with a corresponding slight reduction of the final soot formation. This fact is the consequence of the reduced sooting propensity of pure ethanol.

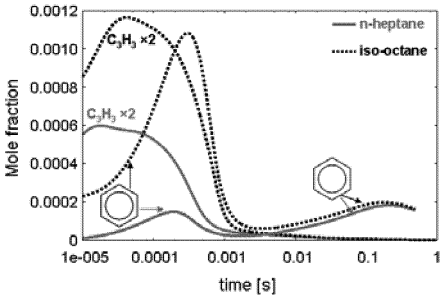

Figure 8. *Benzene and propargyl radical mole fractions at 1500K, P=1 atm, Φ=2.*

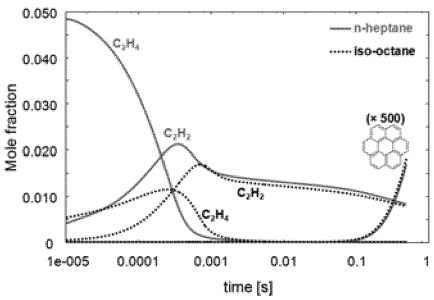

Figure 9. *Ethylene and acetylene mole fractions at 1500K, P=1 atm, Φ=2.*

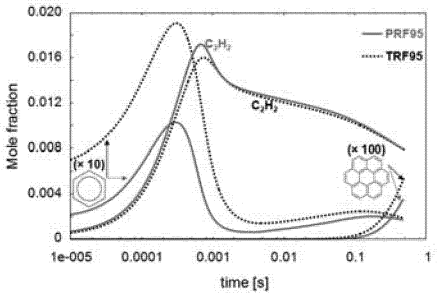

Figure 10. *Benzene, acetylene and coronene from PRF95 and TRF95 at 1500K, 1 atm, Φ=2.*

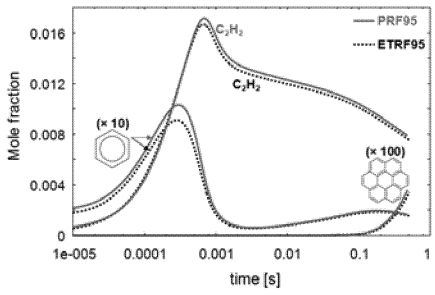

Figure 11. *Benzene, acetylene and coronene from PRF95 and ETRF95 at 1500K, 1 atm, Φ=2.*

These results are very similar to the ones already obtained analysing the formation of soot from droplets of different surrogates, as reported in Figures 4, 5 and 6. The positive effect of ethanol additions to gasolines is proved not only on the basis of an ideal kinetic analysis, but also analyzing the combustion of liquid droplets of different fuel surrogates containing n-heptane, iso-octane and toluene.

Acknowledgements
The Authors wish to thank ENI Spa Refining & Marketing Division for their technical and financial support.

5. References

Buzzi-Ferraris, G. (2007). Numerical Libraries in C++ - Politecnico di Milano, freely available from http://www.chem.polimi.it/homes/gbuzzi.
Buzzi-Ferraris, G. and D. Manca (1998), *Comput Chem Eng*, 22(11), 1595-1621.
Cuoci, A., Mehl, M., Buzzi Ferraris, G., Faravelli, T., Manca, D. and Ranzi, E. (2005a), *Combust. Flame*, **143**:211–226.
Cuoci, A., M. Mehl, T. Paratico, T. Faravelli and E. Ranzi (2005b), *2nd European Combustion Meeting*, Louvain (Belgium), 005_1-005_6.
Gomez, A. and D. E. Rosner (1993), *Combust Sci Tech*, **89**, 335-392.
Kazakov, A., J. Conley and F. L. Dryer (2003), *Combust. Flame*, **134:** 301-314.
Krishna, R. and R. Taylor (1993). *Multicomponent mass transfer*, Wiley.
Marchese, A. J., F. L. Dryer and V. Nayagam (1999), *Combust. Flame*, **116**:432-459
McEnally C. S., D. M. Ciuparu, L. D. Pfefferle (2003), *Combust. Flame* 134: 339–353
Nayagam, V., J. B. Haggard Jr., R. O. Colantonio, A. J. Marchese, F. L. Dryer and F. A. Williams (1998). *AIAA Journal*, **36**, 1369-1378.
Pitz, W.J., Cernansky, N.P., Dryer, F.L., Egolfopulos, F.N., Farrell, J.T., Friend, D.G., and Pitsch, H., *SAE paper* #2007-01-0175 (2007)
Reid,R.C., Prausnitz,J. M., Poling, B.E., *The properties of gases and liquids*, McGraw-Hill 1988.
Sazhin, S. S. (1994), An approximation for the absorption coefficient of soot in a radiating gas, *Fluent Europe (Internal Report)*.
Urban, B. D., Roenlein, K., Kazakov, A., Dryer, F.L., Yozgatligil, A., Choi, M.Y., Manzello, S., Lee, O.K., and Dobashi, R., *Microgavity Sci. Technol.* XV/3: 3-9 (2004).
Yozgatligil,A., Park,S-H, Choi,M.Y., Kazakov,A., Dryer, F.L., *Combust Sci Tech*. 176: 1 (2004).